

See discussions, stats, and author profiles for this publication at: <https://www.researchgate.net/publication/11446667>

Automated Analysis of Nanomolar Concentrations of Phosphate in Natural Waters with Liquid Waveguide

ARTICLE *in* ENVIRONMENTAL SCIENCE AND TECHNOLOGY · APRIL 2002

Impact Factor: 5.33 · DOI: 10.1021/es011094v · Source: PubMed

CITATIONS

100

READS

79

2 AUTHORS, INCLUDING:



[Jia-Zhong Zhang](#)

NOAA Atlantic Oceanographic and Meteorolo...

99 PUBLICATIONS 2,758 CITATIONS

SEE PROFILE

Automated Analysis of Nanomolar Concentrations of Phosphate in Natural Waters with Liquid Waveguide

JIA-ZHONG ZHANG^{*,†,‡} AND JIE CHI^{†,‡}

Cooperative Institute for Marine and Atmospheric Studies, Rosenstiel School of Marine and Atmospheric Science, University of Miami, 4600 Rickenbacker Causeway, Miami, Florida 33149, and Ocean Chemistry Division, Atlantic Oceanographic and Meteorological Laboratory, National Oceanic and Atmospheric Administration, 4301 Rickenbacker Causeway, Miami, Florida 33149

Concentrations of phosphate in natural waters are often below the detection limits of conventional nutrient autoanalyzers, by either gas-segmented continuous-flow analysis or flow injection analysis. A liquid waveguide capillary flow cell has been used to extend the sensitivity of a conventional autoanalyzer for the automated analysis of nanomolar concentrations of phosphate in natural waters. Total reflection of light can be achieved within the liquid core of the flow cell because the refractive index of a cell wall coated with Teflon 1600 is lower than that of water. This property allows the manufacturers to construct long liquid waveguide capillary flow cells in a helical, rather than a linear shape, with compact dimensions. A small sample volume is required because the internal volume of a 2-m long capillary flow cell is only approximately 0.5 cm³. Adaptation of this long flow cell to autoanalyzers significantly enhances the sensitivity of automated colorimetric analysis of phosphate with a molybdenum blue method, allowing for the accurate and precise determination of nanomolar concentrations of phosphate in natural waters. The advantages of this technique are a low detection limit (0.5 nM), a small sample volume (2 mL), high precision (2% at 10 nM levels), and automation for the rapid analysis of a large number of samples.

Introduction

Phosphorus is an essential macronutrient required for living organisms in terrestrial and aquatic environments. In particular, calcium phosphate is a building block for teeth and bones of vertebrates, and adenosine triphosphate is the universal carrier of chemical energy in all living cells (1). As a result, ecosystems are sensitive to the levels of available phosphate. Excessive loadings of phosphate by agriculture runoff and wastewater discharge often result in eutrophication in estuarine and coastal waters (2). Phosphorus is held largely in the earth's crust as a sparingly soluble mineral, such as apatite, fluorapatite, and hydroxyapatite (3). The low solubility of phosphorus-containing minerals and the strong

tendency of dissolved phosphate to absorb onto a solid surface set an upper limit of phosphate concentrations in natural waters at micromolar levels (4–6). The biological uptake of phosphate further depletes its concentrations in surface waters to nanomolar levels. Low levels of available phosphate become a factor limiting the primary production in many aquatic ecosystems (7–10). Simultaneous observations of biological uptake of both nitrogen and phosphorus are critical in understanding the biological response to limiting nutrients. A diurnal cycle of nitrate as a result of photosynthesis has been observed in oligotrophic oceanic waters in response to changes in solar radiation (11). Concurrent observation with a change in phosphate concentration has not been possible because of technical limitations in the ability to quantify in situ changes in phosphate concentrations at nanomolar levels. Highly sensitive phosphate analytical techniques are, therefore, needed to quantify the rate of uptake of phosphate by organisms and to understand its cycling in aquatic environments.

The most common analytical method for determining phosphate concentration is spectrophotometry. The technique relies upon the reaction of phosphate with molybdate in an acidic solution to form a 12-molybdophosphoric acid and its subsequent reduction to the phosphomolybdenum blue complex (12–14), the absorbance of which is readily measured by a spectrophotometer. Over decades, numerous modifications have been made with respect to the reaction temperature, pH, choice of reductants, and potential interferences (15–26). Today, automated gas-segmented continuous-flow analyzers are commonly used for phosphate determination in shipboard or land-based laboratories. However, autoanalyzers utilizing the standard phosphomolybdenum blue method have a detection limit of 50 nM and are unable to accurately quantify the changes in phosphate concentration at nanomolar levels in oligotrophic waters. Consequently, many efforts have been devoted to improve method sensitivity and precision for low-level phosphate analyses. Organic solvents have been used to extract and concentrate phosphomolybdenum blue from aqueous solutions (27). Magnesium hydroxide-induced coprecipitation has also been used to concentrate the sample phosphate in precipitate followed by dissolution in a small volume of HCl solution (28). Both methods can increase sensitivity by an order of magnitude but require a large volume of samples. Moreover, both methods are labor-intensive and time-consuming and are not amenable for automated analyses. Laser-induced thermal lensing colorimetry has been proposed to increase the sensitivity of phosphate analysis (29). This technique, however, requires sophisticated equipment and is not feasible for field analyses.

In spectrophotometry, the absorbance signal, according to the Beer–Lambert law, is proportional to the optical path length of a flow cell filled with sample solution and the concentration of analyte of interest. In addition to optimizing the chemical reaction, increasing the path length of the sample cell is the most feasible approach to enhance the sensitivity of conventional colorimetry. In the 1980s, light-reflective aluminum tape was used to cover the outer surface of a long cell in order to constrain the source light within the long capillary cell. Such long cells suffer serious attenuation of source light and nonlinearity from interference (30, 31). It was not until 1989 when Teflon AF-1600, 1601, and 2400 (DuPont Fluoroproducts, Wilmington, DE) were found to be the only synthesized materials with a refractive index (1.31) lower than that of water (1.33) (32). Total reflection of light within the liquid core surrounded by Teflon AF can be

* Corresponding author phone: (305) 361-4397; fax: (305) 361-4392; e-mail: zhang@aoml.noaa.gov; address: Dr. Jia-Zhong Zhang, OCD/AOML/NOAA, 4301 Rickenbacker Causeway, Miami, FL 33149.

[†] University of Miami.

[‡] National Oceanic and Atmospheric Administration.

Field research programs require an automated analytical system to promptly analyze a large number of samples. Recently, we have successfully incorporated a liquid waveguide capillary flow cell to a gas-segmented continuous-flow autoanalyzer to significantly enhance the sensitivity of shipboard analysis of nitrate, nitrite (45), and iron (46). Using this technique, the detailed diel cycling of nitrate at nanomolar levels in oligotrophic waters was observed for the first time (11). In this study, we extended the application of our analytical system to phosphate analysis and developed a gas-segmented continuous-flow analytical method to determine trace phosphate in natural waters using a conventional autoanalyzer in conjunction with a long liquid waveguide capillary flow cell.

Experimental Section

Liquid Waveguide Capillary Flow Cell (LWCFC). Although LWCFC can be directly constructed with Teflon-AF, it was found that such a cell, due to the porous nature of Teflon AF, was susceptible to adsorption of surface reactive species from aqueous samples. To avoid potential contamination, World Precision Instruments (Sarasota, FL) has designed a novel LWCFC that was made up of capillary quartz tubing, and its outer surface was clad with a layer of Teflon AF-1600 (33, 34). In such a designed LWCFC, the sample has no direct contact with the surface of the Teflon, and LWCFC's inner quartz surface is easy to clean with conventional cleaning reagents, such as dilute HCl or NaOH solutions.

The 2-m long LWCFC is made of quartz capillary tubing with a 550 μm i.d. (World Precision Instruments). Its outer surface is coated with a low refractive index cladding material, Teflon AF-1600, followed by a layer of protective coating. It is looped in three turns and placed in a 30 \times 30 cm metal case for protection. The light pass and sample flow are connected to the LWCFC by T connectors. A detailed description of the connections of LWCC and modification of detector is given elsewhere (45, 47).

Automated Analysis of Phosphate. A gas-segmented continuous-flow colorimetric method was used for the automated determination of phosphate concentrations in natural water. The manifold configuration and flow diagram is shown in Figure 1. The analytical method used is essentially similar to the Murphy and Riley method (15) with modification by Zhang et al. (25). A 12-molybdophosphoric acid is formed from the reaction of phosphate in the sample with molybdate in an acidic solution ($\text{pH} = 1.0$) in the presence of potassium antimony tartrate. The 12-molybdophosphoric acid is subsequently reduced by ascorbic acid to a phosphomolybdenum blue complex. The absorbance of the phosphomolybdenum blue complex is measured at 710 nm. To minimize the sample silicate interference in phosphate analysis, color was developed at room temperature, and no heater is required for this system (25).

Reagents and Standards. Deionized water used for preparing standard and reagents was purified by a distilling unit followed by Millipore Super-Q Plus Water System that produce water with 18 M Ω resistance. To avoid contamination in trace analysis, deionized water was used the day of purification. All samples and reagents were stored in polypropylene bottles, which were ultrasonicated in 1 M HCl

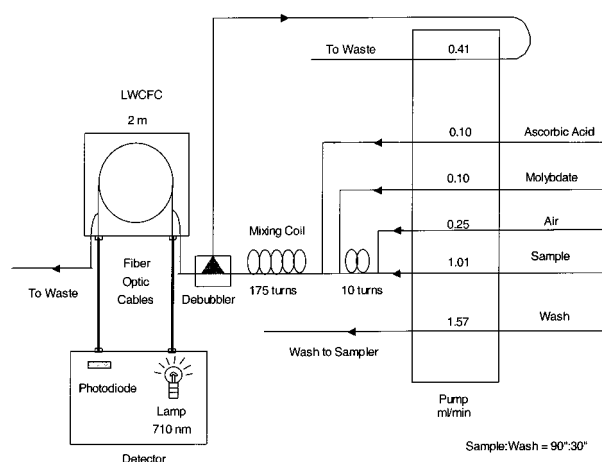


FIGURE 1. Manifold configuration and flow diagram of phosphate analysis with a liquid waveguide capillary flow cell (LWCFC). The detector wavelength is 710 nm, and flow rates are in milliliters per minute.

at 60 °C for 24 h in a clean-air flow bench and were then rinsed three times with deionized water prior to their use.

All reagents used were of analytical grade. Stock antimony potassium tartrate solution was prepared by dissolving 3 g of antimony potassium tartrate ($\text{K}(\text{SbO})\text{C}_4\text{H}_4\text{O}_6 \cdot 1/2\text{H}_2\text{O}$) in 1 L of deionized water. The solution was stored in a dark bottle in a refrigerator. Stock ammonium molybdate solution was prepared by dissolving 2.3 g of ammonium molybdate in 192 mL of 5 N H_2SO_4 solution, then adding 50 mL stock antimony potassium tartrate solution, and diluting to 1 L with deionized water. An aliquot of 100 mL of solution is sufficient for daily analysis. Ascorbic acid solution was prepared daily by dissolving 0.5 g of ascorbic acid and 7 g of sodium dodecyl sulfate ($\text{CH}_3(\text{CH}_2)_{11}\text{OSO}_3\text{Na}$) in 100 mL of deionized water. Sodium dihydrogen phosphate was used to prepare the stock phosphate standard solution (2 mM). The stock solutions were stored in polyethylene bottles at 4 °C in a refrigerator. Working standard solutions were prepared daily from serial dilution of stock solutions with deionized water. Phosphate-free seawater was prepared by the removal of background phosphate in low-nutrient seawater that was collected from the surface of the Gulf Stream. The addition of 1 M NaOH to low-nutrient seawater at a 1:40 v/v ratio produced $\text{Mg}(\text{OH})_2$ precipitate that effectively scavenged background phosphate out of seawater onto $\text{Mg}(\text{OH})_2$ surfaces (28). Precipitation was aged and allowed to settle down overnight. The supernatant was then siphoned as phosphate-free seawater, which was used as wash solution and for the preparation of standards in a seawater matrix.

Results and Discussion

Optimization of Flow Analysis. As discussed previously, the high precision obtainable from gas-segmented continuous-flow analysis is attributed to segmentation gas bubbles that significantly reduce the carryover and sample dispersion (44, 48). To establish a regular bubble pattern and minimize bubble breaking, the addition of a suitable surfactant to the flow stream is a common practice in gas-segmented continuous-flow analysis for achieving a smooth flow with low baseline noise. As a result, a reagent-compatible surfactant should be chosen when adapting a colorimetric method to gas-segmented continuous-flow analysis. Both Dowfax (Dow Chemical Company, Midland, MI) and sodium dodecyl sulfate have been used for phosphate analysis with conventional autoanalyzer (21) and were tested for the suitability for phosphate analysis with a long flow cell. Comparison between Dowfax and sodium dodecyl sulfate indicated that

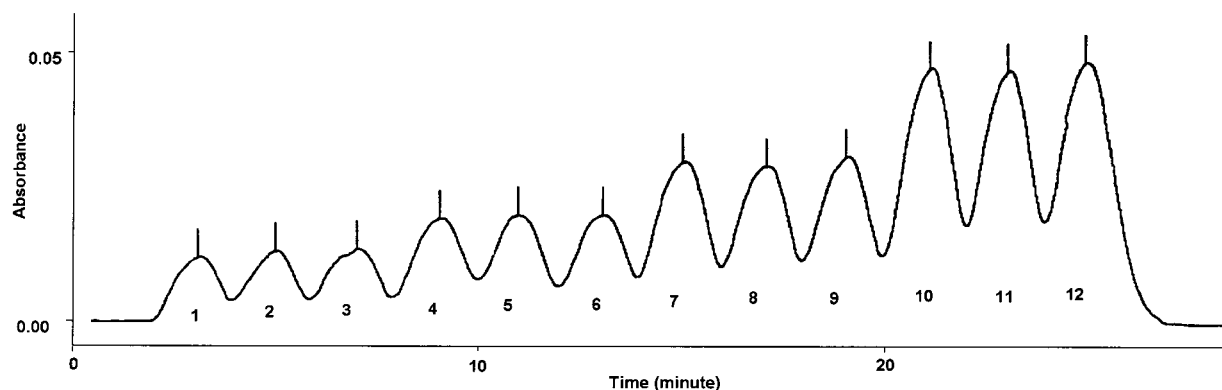


FIGURE 2. Typical output signal of low-level phosphate analysis using LWCFC. Peaks 1–12 are three replicates samples containing phosphate concentrations of 4, 8, 12, and 16 nM, respectively.

sodium dodecyl sulfate is superior to Dowfax with respect to the background absorbance and coating effect. As a result, sodium dodecyl sulfate was chosen as a surfactant for subsequent phosphate analysis.

In gas-segmented continuous-flow analysis, the carryover coefficients are often used to characterize the smooth of flow and effectiveness of the added surfactant in a flow system. The carryover refers to the effect of concentration of a preceding sample upon a subsequent sample in a flow system. A carryover coefficient is often determined by using a high-concentration sample followed by two low-concentration samples or two blanks (HLL scheme) (48). Using sodium dodecyl sulfate as a surfactant, carryover coefficients determined by a high standard followed by two blanks usually produced values of about 0.01. As discussed previously, the small degree of carryover and sample dispersion in the LWCFC system is probably attributed to the small cross section of the capillary flow cell. The internal volume of a 2 m LWCFC with a 550 μm i.d. is approximately 0.5 cm^3 , 30 times larger than an ordinary cell volume of $1.5 \times 10^{-2} \text{ cm}^3$. However, a sample time of 90 s was found to be sufficient in reaching a maximum absorbance output. The performance of the LWCFC is comparable with the ordinary flow cell with respect to the characteristic of carryover and sample dispersion.

In phosphate analysis, molybdate is injected to the flow stream to react with sample phosphate and form a 12-molybdophosphoric acid, which is subsequently reduced by ascorbic acid to phosphomolybdenum blue. Reaction times of phosphate with molybdate prior to reduction by ascorbic acid were investigated to define optimal reaction kinetics. Under a constant flow rate, the reaction times were varied by placing different lengths of mixing coils between injections of molybdate and ascorbic acid. The parameters used for evaluation of optimal conditions are sensitivity, precision, carryover, and intercept in a linear calibration curve. A series of duplicate samples over a range of phosphate concentrations were analyzed under different flow configurations to evaluate the effect on these parameters.

Phosphate signal was obtained when no mixing coil was placed between the injections of these two reagents, indicating a rapid reduction of 12-molybdophosphoric acid by ascorbic acid. An increase in the length of coils placed between the two injections decreases the precision and linearity of the calibration curve. The best precision (2% at 10 nM levels) and linearity were achieved with no mixing coil between the two injections. This suggested that the formation of 12-molybdophosphoric acid is rapid and that its further reduction by ascorbic acid should proceed immediately. To ensure a complete reduction of 12-molybdophosphoric acid by ascorbic acid, a 175-turn mixing coil (7×25 turns) was placed after the injection of ascorbic acid

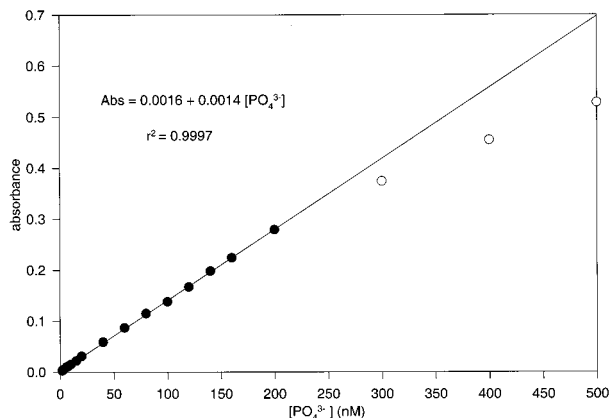


FIGURE 3. Linearity of phosphate determination by gas-segmented continuous-flow analysis with the LWCFC. The open circles indicate the absorbance of phosphate concentration beyond the linear dynamic range and are not used for linear regression.

reagent. A similar sensitivity but deteriorated precision was obtained when a single reagent solution, which was prepared by mixing the molybdate solution with the ascorbic acid solution, was used.

Calibration Characteristics. With such an optimized flow configuration as shown in Figure 1, a typical output signal of automated analysis with LWCFC for low phosphate samples is shown in Figure 2. Using the manifold in Figure 1, the upper limit of linear dynamic range of phosphate analysis is 200 nM (Figure 3). A linear absorbance response to phosphate concentrations below 200 nM can be obtained as

$$\text{Absorbance} = (0.0016 \pm 0.0006) + (0.001391 \pm 0.000006)[\text{PO}_4^{3-}] \text{ (nM)}$$

with $r^2 = 0.9997$ ($n = 15$, standard error = 0.0015). Above this concentration range, the measured absorbances as shown in open circles in Figure 3 are lower than that predicted from the linear relationship. The linear dynamic range of phosphate analysis can be extended by either using a shorter LWCFC or by diluting the sample with deionized water. The latter can easily be done in flow analysis by adding a dilution line to the sample flow in the manifold configuration.

Because reagent solutions are pumping continuously through the flow system and reagent blank signals are usually set to zero in a monochromator, phosphate contamination in reagent solution does not contribute proportionally to the analytical blanks. However, reagent blank does raise the baseline signal. It is desirable to minimize the baseline signal in a flow system because an elevated baseline decreases the

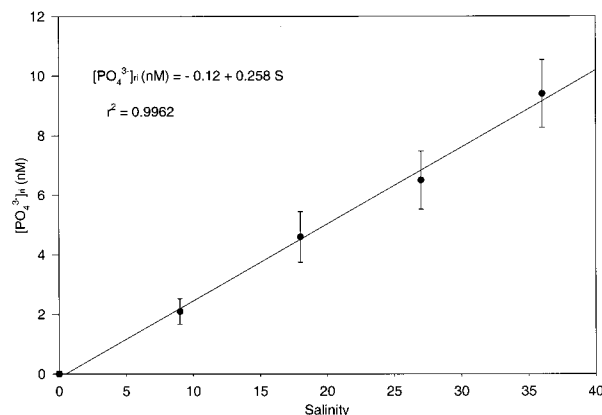


FIGURE 4. Apparent phosphate concentrations due to refractive index interference in the analytical system as a function of sample salinity when deionized water is used as a wash solution.

linear dynamic range of the method and pump pulsing and flow fluctuation cause degradation in the precision at higher baseline levels. For our monochromator equipped with the long liquid waveguide flow cell with the absorbance set to zero when deionized water pumping through the flow cell, a typical baseline for the reagent stream is 0.2 absorbance units. The detection limit of the method is 0.5 nM, which is estimated from 3 times the standard deviation of measurement blanks.

In continuous-flow analysis, differences in the refractive index of the aqueous samples and wash solution can cause interference in absorbance measurements. The effect is more pronounced at the sample/wash solution interface where the concentration, and hence the refractive index gradient, is greatest. If a sample's salinity does not match that of the wash solution and the standards, the absorbance signals must be corrected for the refractive index interference.

As in the conventional continuous-flow analysis, the refractive index of an analytical system using the LWCF

was quantified by measuring the absorbance of water samples of different salinities relative to deionized water. This is achieved by analyzing different salinity waters as phosphate samples using low-nutrient seawater as a wash solution with the exception of the molybdate solution being replaced with a 1 N sulfuric acid solution. The resultant absorbances were converted to phosphate concentrations using a calibration curve constructed based on standard solutions of known phosphate concentrations. The measured refractive index of system is directly proportional to salinity as follows (see Figure 4)

$$[\text{PO}_4^{3-}]_{\text{ri}} = -0.12 + 0.258 S \quad (r^2 = 0.9962, n = 5)$$

where $[\text{PO}_4^{3-}]_{\text{ri}}$ is a correction for refractive index interference for sample phosphate concentration in nM and S is salinity of samples. To avoid the significant correction for refractive index interference for low-level phosphate samples, matching the wash solution with sample in salinity and using phosphate-free seawater is recommended.

Application to Natural Water Samples. This method has been used to determine the concentrations of dissolved phosphate in Florida Bay, FL. The bay is a triangular shape and bounded to the north by the Florida Peninsula and to the south and east by the reef ridge of the Florida Keys (Figure 5). The western margin of the bay is open to the Gulf of Mexico. Biogenic calcium carbonate is major component of the sediment (>90%) in the Florida Bay. The resuspension of carbonate sediments driven by wind and tidal mixing in shallow water (average water depth ~2 m) of the Florida Bay effectively scavenges the phosphate from seawater onto carbonate sediments and depletes the seawater phosphate concentrations to nanomolar levels. Conventional autoanalyzers are not sensitive enough to accurately quantify the phosphate concentration in such carbonate-dominated, shallow-water ecosystems.

A total of 40 stations were occupied during a survey cruise, and surface water samples were collected from Florida Bay

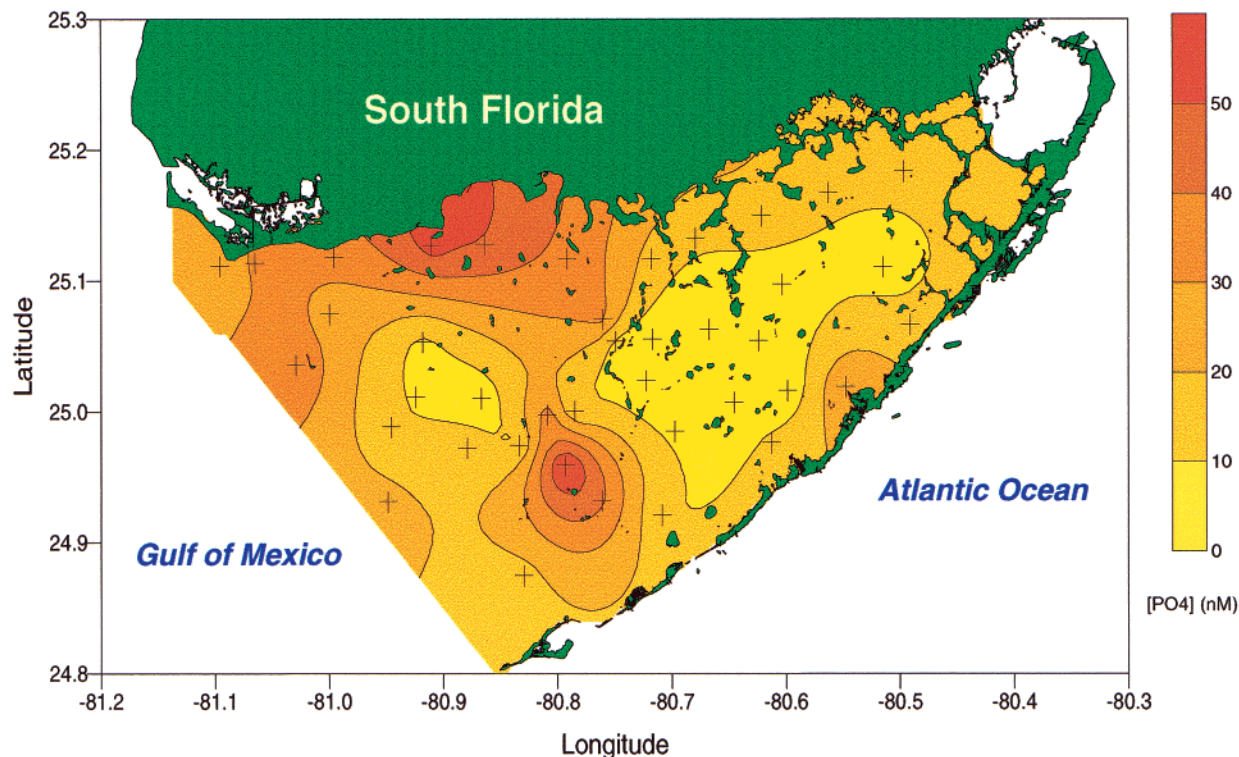


FIGURE 5. Spatial distribution of dissolved phosphate in Florida Bay water. A total of 40 stations were sampled during the survey.

TABLE 1. Concentrations of Dissolved Phosphate in Surface Water of Florida Bay Determined by Gas-Segmented Continuous-Flow Analysis with a LWCFC^a

station	latitude (°N)	longitude (°W)	[PO ₄ ³⁻] (nM)
1	25.1840	80.4968	12.5
2	25.1673	80.5623	12.2
3	25.1498	80.6212	17.4
4	25.1329	80.6791	12.1
5	25.1169	80.7179	16.2
6	25.0708	80.7604	33.1
7	25.1171	80.7915	36.4
8	25.1283	80.8639	49.2
9	25.1266	80.9102	54.6
10	25.1182	80.9957	33.6
11	25.0746	81.0002	25.4
12	25.1139	81.0648	32.2
13	25.1118	81.0959	21.0
14	25.0355	81.0290	39.1
15	24.9313	80.9485	23.2
16	24.8748	80.8293	15.8
17	24.9215	80.7085	10.8
18	24.9765	80.6125	12.1
19	25.0191	80.5473	30.4
20	25.0668	80.4909	12.5
21	25.1110	80.5145	6.9
22	25.0977	80.6034	3.4
23	25.0547	80.6242	1.6
24	25.0633	80.6672	1.6
25	25.0558	80.7170	1.8
26	25.0240	80.7222	2.0
27	25.0538	80.7491	7.2
28	25.0004	80.7847	9.3
29	24.9975	80.8094	35.3
30	24.9745	80.8335	8.7
31	25.0102	80.8668	4.0
32	25.0111	80.9243	9.3
33	25.0531	80.9180	7.1
34	24.9883	80.9457	11.2
35	24.9722	80.8788	16.7
36	24.9589	80.7934	63.8
37	24.9320	80.7612	42.0
38	24.9853	80.6974	7.8
39	25.0073	80.6457	2.6
40	25.0163	80.5985	2.1

^aA total of 40 stations were occupied and sampled between November 13–14, 2000.

during November 13–14, 2000. Samples were filtered immediately after collection through a 0.45 μ m Nuclepore filters to remove particulate matter and stored in plastic bottles in a cooler at ca. 4 °C. Water samples were transported to the laboratory and analyzed within 2 days of sample collection. To analyze these samples, phosphate standard solutions were prepared in phosphate-free seawater by the magnesium hydroxide precipitation technique as mentioned previously. This phosphate-free seawater was also used as the wash solution to match sample salinity and, therefore, to avoid any refractive index interferences. Phosphate concentrations in Florida Bay water range from 1.6 to 63.8 nM (Table 1). The spatial variations of dissolved phosphate in Florida Bay as shown in Figure 5 are consistent with distribution of sedimentary phosphorus pools (Zhang et al.; unpublished data), suggesting that concentrations of dissolved phosphate in shallow Florida Bay water are mainly regulated by the phosphate buffering mechanism of carbonate sediments (49). The large spatial gradients are mainly due to numerous mud banks that divide the bay into several sub-basins and limit water exchange between sub-basins. Higher concentrations of phosphate in the western bay relative to the eastern bay are in part due to the supply of phosphate from the west Florida shelf current. This current carries phosphate-laden water, which is originated from runoff in phosphorus mining

areas in the central Florida, along the west Florida coast. Low concentrations of phosphate (<10 nM) were found in the eastern basin where it receives freshwater input from the Everglades that contain a relatively low phosphate concentration as a result of the rapid retention of phosphate by carbonate soil and uptake by vegetation while water flows through the Everglades.

In summary, the incorporation of a liquid waveguide capillary flow cell to a conventional autoanalyzer significantly enhances the sensitivity of the gas-segmented continuous-flow colorimetric analysis. The advantages of this technique are a low detection limit, high precision, and automation for rapid analyses of a large number of samples. Our results have demonstrated the feasibility of this technique for the determination of nanomolar concentrations of phosphate in natural waters.

Acknowledgments

The authors thank C. Fischer and C. Kelble for collecting water samples in Florida Bay. This work was supported by National Oceanic and Atmospheric Administration (NOAA) South Florida Ecosystem Restoration Prediction and Modeling Program under the Coastal Ocean Program and Global Carbon Cycle program under the Climate and Global Change Program. This research was carried out under the auspices of the Cooperative Institute for Marine and Atmospheric Studies (CIMAS), a joint institute of the University of Miami and the National Oceanic and Atmospheric Administration, cooperative agreement No. NA67RJ0149.

Literature Cited

- (1) Westheimer, F. H. *Science* **1987**, *235*, 1173–1178.
- (2) Ryther, J. H.; Dunstan, W. M. *Science* **1971**, *171*, 1008–1013.
- (3) *Environmental Phosphorus Handbook*; Griffith, E. J., Beeton, A. M., Spencer, J. M., Michell, D. J., Eds.; Wiley & Sons: New York, 1973.
- (4) Kramer, J. R. *Science* **1964**, *146*, 637–638.
- (5) Follmi, K. B. *Earth–Sci. Rev.* **1996**, *40*, 55–124.
- (6) Froelich, P. N.; Bender, M. L.; Luedtke, N. A.; Hearsh, G. R.; DeVries, T. *Am. J. Sci.* **1982**, *282*, 474–511.
- (7) Smith, S. V.; Atkinson, M. J. *Nature* **1984**, *307*, 626–627.
- (8) Smith, S. V. *Limnol. Oceanogr.* **1984**, *29*, 1149–1160.
- (9) Schindler, D. W. *Science* **1977**, *195*, 260–262.
- (10) Krom, M. D.; Kress, N.; Brenner, S.; Gordon, L. I. *Limnol. Oceanogr.* **1991**, *36*, 424–432.
- (11) Zhang, J.-Z.; Wanninkhof, R.; Lee, K. *Geophys. Res. Lett.* **2001**, *28*, 1579–1582.
- (12) Murphy, J.; Riley, J. P. *J. Mar. Biol. Assoc. U.K.* **1958**, *37*, 9–14.
- (13) Boltz, D. F. In *Analytical Chemistry of Phosphorus Compounds*; Hammann, M., Ed.; Wiley: New York, 1972; pp 9–65.
- (14) Boltz, D. F.; Lueck, C. H.; Jakubiec, R. J. In *Colorimetric Determination of nonmetals, Chemical Analysis*, 2nd ed.; Boltz, D. F., Howell, J. A., Eds.; Wiley: New York, 1978; Vol. 8, pp 337–369.
- (15) Murphy, J.; Riley, J. P. *Anal. Chim. Acta* **1962**, *27*, 31–36.
- (16) Chan, K. M.; Riley, J. P. *Deep–Sea Res.* **1966**, *13*, 467–471.
- (17) Crouch, S. R.; Malmstadt, H. V. *Anal. Chem.* **1967**, *39*, 1084–1089.
- (18) Going, J. E.; Eisenreich, S. J. *Anal. Chim. Acta* **1974**, *70*, 95–106.
- (19) Broberg, O.; Pettersson, K. *Hydrobiologia* **1988**, *170*, 45–59.
- (20) Pai, S.-C.; Yang, C.-C. *Anal. Chim. Acta* **1990**, *229*, 115–120.
- (21) Blomqvist, S.; Hjellstrom, K.; Sjosten, A. *Int. J. Environ. Anal. Chem.* **1993**, *54*, 31–43.
- (22) Drummond, L.; Maher, W. *Anal. Chim. Acta* **1995**, *302*, 69–74.
- (23) Blomqvist, S.; Westin, S. *Anal. Chim. Acta* **1998**, *358*, 245–254.
- (24) Sjosten, A.; Blomqvist, S. *Water Res.* **1997**, *31*, 1818–1823.
- (25) Zhang, J.-Z.; Fischer, C. J.; Ortner, P. B. *Talanta* **1999**, *49*, 293–304.
- (26) Zhang, J.-Z.; Fischer, C. J.; Ortner, P. B. *Int. J. Environ. Anal. Chem.* **2001**, *80*, 61–73.
- (27) Stephens, K. *Limnol. Oceanogr.* **1963**, *8*, 361–362.
- (28) Karl, D.; Tien, G. *Limnol. Oceanogr.* **1992**, *37*, 105–116.
- (29) Fujiwara, K.; Lei, W.; Uchiki, H.; Shimokoshi, F.; Fuwa, K.; Kobayashi, T. *Anal. Chem.* **1982**, *54*, 2026–2029.
- (30) Lei, W.; Fujiwara, K.; Fuwa, K. *Anal. Chem.* **1983**, *55*, 951–955.

- (31) Fuwa, K.; Lei, W.; Fujiwara, K. *Anal. Chem.* **1984**, *56*, 1640–1644.
- (32) Buck, W. H.; Resnick, P. R. Dupont Technical Product Information, 1993.
- (33) Liu, S. Y. Improved aqueous fluid core waveguide. U.S. Patent 5,570,447, 1996.
- (34) Liu, S. Y. Rigid aqueous fluid core light guide and application thereof. U.K. Patent 2,284,904, 1997.
- (35) Dasgupta, P. K.; Genfa, Z.; Poruthoor, S. K.; Caldwell, S.; Dong, S.; Liu, S. Y. *Anal. Chem.* **1998**, *70*, 4661–4669.
- (36) Dasgupta, P. K.; Genfa, Z.; Li, J.; Boring, C. B.; Jambunathan, S.; Al-Horr, R. *Anal. Chem.* **1999**, *71*, 1400–1407.
- (37) Li, J.; Dasgupta, P. K.; Genfa, Z. *Talanta* **1999**, *50*, 617–623.
- (38) Holz, M.; Dasgupta, P. K.; Genfa, Z. *Anal. Chem.* **1999**, *71*, 2934–2938.
- (39) Song, L.; Liu, S. Y.; Zhelyaskov, V.; El-Sayed, M. A. *Appl. Spectrosc.* **1998**, *52*, 1364–1367.
- (40) D'Sa, E. J.; Seward, R. G.; Vodacek, A.; Blough, N. V.; Phinney, D. *Limnol. Oceanogr.* **1999**, *44*, 1142–1148.
- (41) Waterbury, R. D.; Yao, W.; Byrne, R. H. *Anal. Chim. Acta* **1997**, *357*, 99–102.
- (42) Yao, W.; Byrne, R. H.; Waterbury, R. D. *Environ. Sci. Technol.* **1998**, *32*, 2646–2649.
- (43) Yao, W.; Byrne, R. H. *Talanta* **1999**, *48*, 277–282.
- (44) Byrne, R. H.; Yao, W.; Kaltenbacher, E.; Waterbury, R. D. *Talanta* **2000**, *50*, 1307–1312.
- (45) Zhang, J.-Z. *Deep-Sea Res.* **2000**, *47*, 1157–1171.
- (46) Zhang, J.-Z.; Kelble, C.; Millero, F. J. *Anal. Chim. Acta* **2001**, *438*, 49–57.
- (47) Liquid Waveguide Capillary Cell (LWCC), World Precision Instruments Technical Data Sheet; World Precision Instruments: Sarasota, FL, 1999.
- (48) Zhang, J.-Z. *J. Automatic Chem.* **1997**, *19*, 205–212.
- (49) Froelich, P. N. *Limnol. Oceanogr.* **1988**, *33*, 649–668.

Received for review June 26, 2001. Revised manuscript received November 1, 2001. Accepted November 12, 2001.

ES011094V